EUKARYOTIC CELL, Dec. 2006, p. 2120–2127 Vol. 5, No. 12
1535-9778/06/$08.00+0 doi:10.1128/EC.00121-06

Identification of Translational Regulation Target Genes during Filamentous Growth in *Saccharomyces cerevisiae*: Regulatory Role of Caf20 and Dhh1▽

Young-Un Park, Hyangsuk Hur, Minhan Ka, and Jinmi Kim*

Department of Microbiology, School of Bioscience and Biotechnology, Chungnam National University, Daejeon 305-764, Republic of Korea

Received 21 April 2006/Accepted 2 October 2006

The dimorphic transition of yeast to the hyphal form is regulated by the mitogen-activated protein kinase and cyclic AMP-dependent protein kinase A pathways in *Saccharomyces cerevisiae*. Signaling pathway-responsive transcription factors such as Ste12, Tec1, and Flo8 are known to mediate filamentation-specific transcription. We were interested in investigating the translational regulation of specific mRNAs during the yeast-to-hyphal-form transition. Using polyribosome fractionation and RT-PCR analysis, we identified *STE12*, *GPA2*, and *CLN1* as translation regulation target genes during filamentous growth. The transcript levels for these genes did not change, but their mRNAs were preferentially associated with polyribosomes during the hyphal transition. The intracellular levels of Ste12, Gpa2, and Cln1 proteins increased under hyphal-growth conditions. The increase in Ste12 protein level was partially blocked by mutations in the *CAF20* and *DHH1* genes, which encode an eIF4E inhibitor and a decapping activator, respectively. In addition, the *caf20* and *dhh1* mutations resulted in defects in filamentous growth. The filamentation defects caused by *caf20* and *dhh1* mutations were suppressed by *STE12* overexpression. These results suggest that Caf20 and Dhh1 control yeast filamentation by regulating *STE12* translation.

The cellular morphology of diploid *Saccharomyces cerevisiae* frequently switches between the yeast and filamentous forms depending on nutritional signals (16). Several signal transduction modules, including the mitogen-activated protein kinase (MAPK) cascade and the cyclic AMP-dependent protein kinase A (PKA) pathway, are known to participate in this switch (14, 21, 31, 36). The MAPK cascade involves Ste20, Ste11, Ste7, Kss1, and the transcription factors Ste12 and Tec1 (15, 21, 29, 30). The PKA pathway involves Gpr1, Gpa2, Ras2, Tpk2, and the transcription factors Flo8 and Sfl1 (22, 26, 31, 32). These signaling pathways control the transcription of a number of filamentation-specific genes, including *FLO11* (19, 23, 29).

Although the signaling pathways and transcriptional regulation of yeast filamentous growth have been studied in considerable detail, little is known about translational regulation related to the transition from the yeast to the filamentous form. In this study, we searched for specific mRNAs that are preferentially translated during the yeast-to-hyphal-form transition. Genome-wide analysis of mRNA translation profiles indicates that the loading of ribosomes onto individual mRNA species varies broadly (20, 28). The association of mRNA transcripts in polyribosomes reflects the rate of synthesis of their corresponding proteins (3, 45). By purifying polyribosome fractions and employing RT-PCR analysis, we found that the mRNA transcripts of *STE12*, *GPA2*, and *CLN1* were preferentially recruited to polyribosomes during filamentation compared to during normal vegetative growth, even though their levels in the total cell extracts were not changed. Consistently, the protein levels of Ste12, Gpa2, and Cln1 also increased during filamentation. The up-regulation of *STE12* mRNA translation during filamentous growth appeared to be partly dependent on *CAF20* and *DHH1*, which encode an eIF4E (the cap-binding protein) inhibitor and an mRNA decapping activator, respectively. Both *CAF20* and *DHH1* were shown to be important for filamentous growth in yeast.

MATERIALS AND METHODS

Strains, plasmids, and growth conditions. The *S. cerevisiae* strains and plasmids used in this study are listed in Table 1. Standard yeast media were prepared using the established procedure (1). Synthetic low-ammonium medium (SLAD) was prepared as described previously (16). 5-FOA (5-fluoro-orotic acid) medium was composed of 0.67% yeast nitrogen without amino acid, 2% dextrose, and 0.1% 5-FOA (1). Standard methods of yeast transformation and genetic crosses were used for the constructions of all strains.

Cell lysis and polyribosome fractionation. Yeast cells were grown at 30°C in YEPD (yeast extract-peptone-dextrose) or SLAD to an A_{600} of 0.8 to 1.0. Prior to cell collection, cycloheximide was added to a final concentration of 50 μg/ml. Cells were pelleted by centrifugation and washed with 1/30 culture volume of breaking buffer A (BBA; 20 mM Tris-Cl [pH 7.5], 50 mM NaCl, 10 mM $MgCl_2$, 1 mM dithiothreitol, 50 μg/ml cycloheximide, and 20 μg/ml heparin) on ice (34). Cells were resuspended in 1.5 cell volumes of BBA and lysed by vortexing in the presence of 1 volume of glass beads. Lysates were clarified by centrifugation at 4,200 rpm for 5 min, and the supernatants were centrifuged at 13,000 rpm for 20 min. Twenty-five A_{260} units of lysates were fractionated on 5-to-45% sucrose gradients as described previously (12). Gradients were centrifuged at 35,000 rpm in an SW41 rotor (Beckman) at 4°C for 3.5 h and were then fractionated with monitoring of A_{254}.

RNA analysis and RT-PCR. Total RNA was isolated from each fraction with an RNeasy kit (QIAGEN). cDNA synthesis was performed using 20 μg/ml RNA in 10 μg/ml oligo(dT), 50 mM Tris-Cl (pH 8.3), 75 mM KCl, 3 mM $MgCl_2$, 10 mM dithiothreitol, 2.5 mM deoxynucleoside triphosphates (dNTPs), and Moloney murine leukemia virus reverse transcriptase (Gibco BRL). Reactions were car-

* Corresponding author. Mailing address: Department of Microbiology, School of Bioscience and Biotechnology, Chungnam National University, Yuseong-Gu, Gung-Dong 220, Daejeon 305-764, Republic of Korea. Phone: 82-42-821-6416. Fax: 82-42-822-7367. E-mail: jmkim@cnu.ac.kr.

▽ Published ahead of print on 13 October 2006.

TABLE 1. Strains and plasmids used in this study

Strain or plasmid	Genotype	Source or reference
Strains[a]		
10560-2B	*MAT***a** *ura3-52 his3::hisG leu2::hisG*	G. R. Fink
10560-5B	*MAT*α *ura3-52 trp1::hisG leu2::hisG*	G. R. Fink
JK353	*MAT***a**/*MAT*α *ura3-52/ura3-52 his3::hisG/+ trp1::hisG/+ leu2::hisG/leu2::hisG*	This laboratory
JK354	*MAT***a**/*MAT*α *ura3-52/ura3-52 his3::hisG/+ trp1::hisG/+ leu2::hisG/leu2::hisG kem1::LEU2/kem1::LEU2*	This laboratory
JK371	*MAT***a** *ura3-52 his3::hisG leu2::hisG FLO11::HA*	This work
JK372	*MAT***a** *ura3-52 his3::hisG leu2::hisG GPA2::HA*	This work
JK373	*MAT***a** *ura3-52 his3::hisG leu2::hisG STE12::HA*	This work
JK374	*MAT***a** *ura3-52 his3::hisG leu2::hisG CLN1::HA*	This work
JK375	*MAT***a** *ura3-52 his3::hisG leu2::hisG FLO8::HA*	This work
JK376	*MAT***a**/*MAT*α *ura3-52/ura3-52 his3::hisG/+ trp1::hisG/leu2::hisG/leu2::hisG FLO11/FLO11::HA*	This work
JK377	*MAT***a**/*MAT*α *ura3-52/ura3-52 his3::hisG/+ trp1::hisG/+ leu2::hisG/leu2::hisG GPA2/GPA2::HA*	This work
JK378	*MAT***a**/*MAT*α *ura3-52/ura3-52 his3::hisG/+ trp1::hisG/+ leu2::hisG/leu2::hisG STE12/STE12::HA*	This work
JK379	*MAT***a**/*MAT*α *ura3-52/ura3-52 his3::hisG/+ trp1::hisG/+ leu2::hisG/leu2::hisG CLN1/CLN1::HA*	This work
JK380	*MAT***a**/*MAT*α *ura3-52/ura3-52 his3::hisG/+ trp1::hisG/+ leu2::hisG/leu2::hisG FLO8/FLO8::HA*	This work
JK381	*MAT***a** *ura3-52 his3::hisG leu2::hisG caf20::LEU2*	This work
JK383	*MAT***a**/*MAT*α *ura3-52/ura3-52 his3::hisG/+ trp1::hisG/+ leu2::hisG/leu2::hisG caf20::LEU2/caf20::LEU2*	This work
JK384	*MAT***a** *ura3-52 his3::hisG leu2::hisG tif1::LEU2*	This work
JK386	*MAT***a**/*MAT*α *ura3-52/ura3-52 his3::hisG/+ trp1::hisG/+ leu2::hisG/leu2::hisG tif1::LEU2/tif1::LEU2*	This work
JK387	*MAT***a** *ura3-52 his3::hisG leu2::hisG dhh1::LEU2*	This work
JK389	*MAT***a**/*MAT*α *ura3-52/ura3-52 his3::hisG/+ trp1::hisG/+ leu2::hisG/leu2::hisG dhh1::LEU2/dhh1::LEU2*	This work
Plasmids		
pJI255	*STE12-HA URA3 CEN*	This work
pJI256	*CLN1-HA URA3 CEN*	This work
pJI257	*FLO8-HA URA3 CEN*	This work
pJI274	*STE12-HA 2*μ *ARS URA3*	This work
pJI276	*CAF20 URA3 CEN*	This work
pJI277	*DHH1 URA3 CEN*	This work
YEp355-FLO11::lacZ	*FLO11::lacZ URA3 2*μ	37
pRS426	*2*μ *ARS URA3*	6
pRS316	*CEN ARS URA3*	42

[a] All yeast strains are derived from the Σ1278b background.

ried out at 37°C for 1 h and followed by heat inactivation at 75°C for 30 min. Each PCR was performed using 5 μl of the cDNA reaction mixture, 2.5 mM dNTPs, 1 unit of *Taq* polymerase, and a pair of gene-specific PCR primers (40 pmol). The amplification was carried out through 30 cycles at 94°C for 30 s, at 52°C for 30 s, and at 72°C for 50 s.

Tagging genes with HA. For tagging target genes with three hemagglutinins, we used an HA-URA3-HA cassette of the pQF296.10 plasmid as described previously (17). The HA integration sites of Flo8-HA and Flo11-HA proteins were as described previously (17, 22). The HA tagging of Gpa2-HA, Ste12-HA, and Cln1-HA proteins was C terminal (see Fig. 2A). The HA-URA3-HA region was PCR amplified using the DNA of the pQF296.10 plasmid as a template and a pair of primers for each target gene. The PCR products were transformed into the 10560-2B strain. Integration of a HA-URA3-HA cassette at each target open reading frame was confirmed by PCR analysis. The URA3 pop-outs from homologous recombination were selected on a 5-FOA plate.

Immunoblot analysis. Total protein preparation and immunoblotting were conducted as previously described (18). HA-tagged proteins were detected with the anti-HA monoclonal antibody 12CA5 (1:1,000 dilution; Boehringer Mannheim). The tubulin proteins were detected using an Anti-Tubulin Cocktail (InnoGenex). HRP-conjugated anti-mouse antibody was utilized as a secondary antibody.

Northern blot analysis. Total RNA was prepared as previously described (10). Twenty micrograms of total yeast RNA was fractionated by electrophoresis through a 1.0% formaldehyde gel and was subsequently transferred to a Nytran membrane (Hoefer). Blotting was performed as described elsewhere (38). The PCR products of *FLO11* (ORF 3541 to 4074), *GPA2* (408 to 1164), *STE12* (1095 to 1759), *CLN1* (428 to 1165), *FLO8* (1081 to 1979), and *ACT1* (49 to 770) were used as probes. Probes were labeled with a Random Prime labeling system (Amersham).

Construction of deletion mutants. Deletion mutations of *CAF20*, *DHH1*, and *TIF1* were constructed using PCR-based gene disruption methods (27, 44). The disruption marker *LEU2* was PCR amplified using primers containing a 51-bp sequence homologous to the target gene and an 18-bp sequence from the *LEU2* marker. The PCR products were transformed into a haploid strain of the **a** or α mating type. Integration of *LEU2* at each gene was confirmed by PCR analysis of genomic DNA from each transformant.

RESULTS

***STE12*, *GPA2*, and *CLN1* mRNA transcripts are preferentially recruited to polyribosomes under filamentous-growth conditions.** Little is known about the translational regulation of specific mRNAs during the yeast-to-hyphal-form transition. Based on the finding that actively translated mRNAs are as-

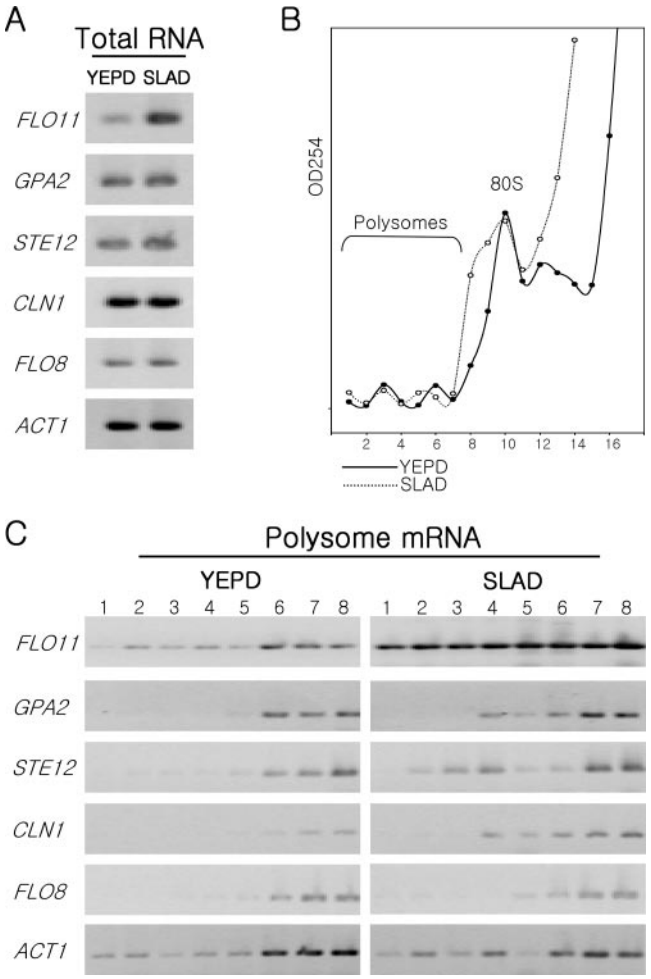

FIG. 1. Polyribosomal profiles of *FLO11*, *GPA2*, *STE12*, *CLN1*, and *FLO8* mRNAs in yeast and pseudohyphal cultures. (A) Total RNAs of *FLO11*, *GPA2*, *STE12*, *CLN1*, and *FLO8* from YEPD (yeast form) and SLAD (pseudohyphal-form) cultures analyzed by RT-PCR. (B) Polyribosome fractionations. Cell lysates from YEPD or SLAD cultures were analyzed by sucrose gradient sedimentation at 35,000 rpm at 4°C for 3.5 h. (C) RT-PCR analysis of *FLO11*, *GPA2*, *STE12*, *CLN1*, and *FLO8* mRNAs from polyribosomal fractions. Lanes 1 to 8 correspond to the fraction numbers in panel B. RT-PCR was performed with a set of gene-specific primers.

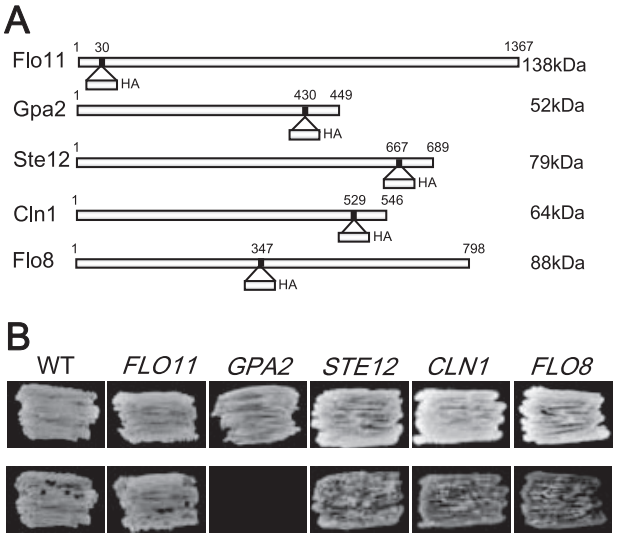

FIG. 2. Construction of HA-tagged strains. (A) Structures of Flo11-HA, Gpa2-HA, Ste12-HA, Cln1-HA, and Flo8-HA proteins. The HA integration site of each construction is indicated. (B) Functional assays of HA-tagged genes. Haploid invasive phenotypes were tested with patches of yeast strains (wild-type strain 10560-2B and HA-tagged strains JK371 to JK375) on solid-agar plates. After incubation, the plates were photographed before (top) and after (bottom) the cells were washed.

sociated with polyribosomes, we analyzed the polyribosomal mRNAs and searched for genes actively translated during hyphal induction. A diploid yeast strain was cultured in either YEPD medium (yeast form) or SLAD (pseudohyphal form) at 30°C for 8 h. At this time point, cells in SLAD are in the early stage of the hyphal transition. This is sufficient to induce hyphal-form-specific gene expression. Total cellular mRNAs were fractionated through a 5-to-45% sucrose gradient, and the abundance of target mRNAs in polyribosomal fractions was analyzed by RT-PCR using gene-specific primers (Fig. 1). The specific mRNA molecules examined include those of two protein kinases (Ste20 and Ste11), five transcription factors (Ste12, Tec1, Flo8, Msn1, and Mss11), a cyclin (Cln1), two membrane-bound signaling molecules (Mep2 and Gpa2), and the cell surface protein Flo11 (13, 14, 24, 26). As shown previously (23), the levels of *FLO11* total RNAs were higher under conditions promoting hyphal growth than conditions promoting yeast growth (Fig. 1A). Accordingly, polyribosomal *FLO11* mRNAs were more abundant in the hyphal culture than the yeast culture (Fig. 1C). Importantly, we found that even though the mRNA levels of *STE12*, *GPA2*, and *CLN1* were not induced under nitrogen starvation conditions (Fig. 1A), these transcripts were enriched in the polyribosomal fractions (Fig. 1C). Total and polysomal levels of *FLO8* mRNA did not change during the yeast-to-hyphal-form transition. Similarly, the transcripts of six other genes (*STE20*, *STE11*, *TEC1*, *MSN1*, *MSS11*, and *MEP2*) were not enriched in the polyribosomal fractions (data not shown). These results suggest that the mRNA of *STE12*, *GPA2*, and *CLN1* were preferentially recruited to polyribosomes for translation during the yeast pseudohyphal differentiation.

Ste12, Gpa2, and Cln1 protein levels increase during filamentous growth. To determine whether the levels of Ste12, Gpa2, and Cln1 proteins increase during the yeast-to-hyphal-form transition, we inserted the HA epitope into the chromosome copy of the *FLO11*, *STE12*, *GPA2*, *CLN1*, and *FLO8* genes in a haploid strain (see Materials and Methods). All of the HA-tagged genes except *GPA2* appeared to be functional in the filamentous phenotype, as assayed by a haploid invasive-growth test (Fig. 2). Diploid strains, which were constructed by mating the HA-tagged strains with the opposite mating type, behaved like a wild-type strain in a pseudohyphal-growth test (data not shown).

HA-tagged diploid strains were grown to the late exponential phase. The cultures were then shifted to filamentation-inducing medium (SLAD), and total protein was isolated after 2, 4, and 8 h. At the 4- and 8-h time points, the level of Flo11-HA protein in the hyphal culture was higher than in the

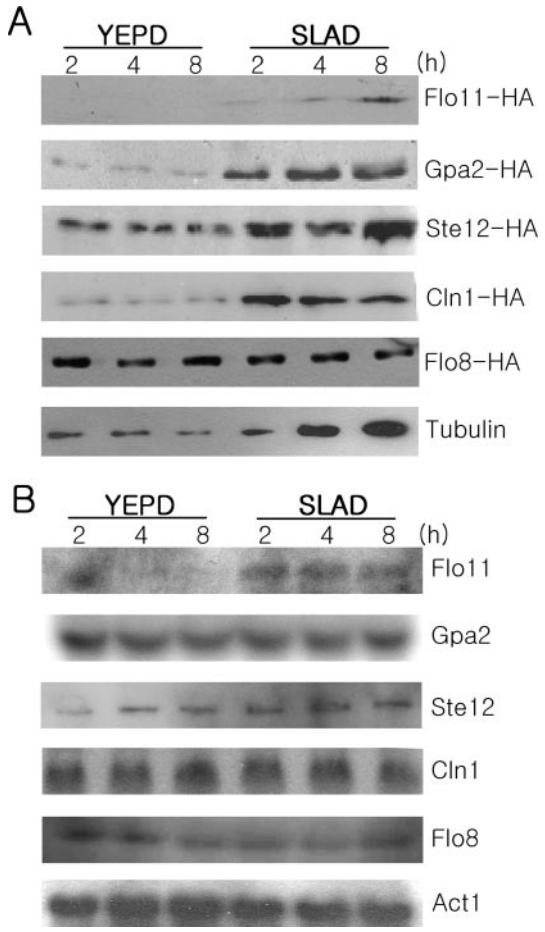

FIG. 3. Increased levels of Gpa2, Ste12, and Cln1 proteins during the pseudohyphal transition. (A) Western blots of Flo11-HA (JK376), Gpa2-HA (JK377), Ste12-HA (JK378), Cln1-HA (JK379), and Flo8-HA (JK380) strains in YEPD medium or SLAD. Tubulins, commonly used as a loading control, showed an increase in the protein level in SLAD. Flo8-HA showed a constant level of proteins. (B) Northern blots of Flo11-HA, Gpa2-HA, Ste12-HA, Cln1-HA, and Flo8-HA strains in YEPD medium or SLAD. Act1 is a loading control.

yeast form (Fig. 3A). Northern blotting showed that the level of *FLO11* transcripts was also increased in the hyphal culture (Fig. 3B). These results confirm the previous finding that *FLO11* induction is at the transcriptional level. The levels of Ste12-HAp, Gpa2-HAp, and Cln1-HAp increased during pseudohyphal growth, but their transcript levels remained unchanged (Fig. 3B). These results correlated with an enrichment of *STE12*, *GPA2*, and *CLN1* mRNAs in the polyribosome fractions. The level of Flo8-HAp was the same under yeast and pseudohyphal-form growth conditions. These results suggest that expression of *STE12*, *GPA2*, and *CLN1* is controlled at the translational level during the yeast-to-pseudohyphal-form transition.

Caf20 and Dhh1 regulate *STE12* expression during filamentous growth. We next considered whether any components of the translational machinery play a regulatory role in expression of *STE12*. Deletion mutations of *CAF20* (eIF4E-binding protein) or *TIF1* (eIF4A) were constructed in strain Σ1278b, commonly used for studying filamentous growth. At the early step of translation initiation, the cap-binding protein eIF4E binds to m^7G caps at the 5′ termini of mRNA and subsequently associates with eIF4G (33, 43). Caf20 is known to compete with eIF4G for binding to eIF4E and to inhibit cap-dependent translation (2, 9, 35). The RNA helicase eIF4A is another binding partner of eIF4G and is thought to unwind the 5′ secondary structure of mRNA. Two duplicate genes, *TIF1* and *TIF2*, encode eIF4A, and disruption of both is lethal to the cell (39). As shown in Fig. 4A, *caf20*/*caf20* and *tif1*/*tif1* diploid mutant strains showed lower levels of Ste12-HAp than the wild type under filamentous-growth conditions. The relative levels of Ste12p were 0.53 for *caf20* and 0.74 for *tif1* (Fig. 4B). The effects of the *caf20* or *tif1* mutations did not appear to be due to general translational repression in the filamentation-inducing medium, because these mutations did not affect the level of Cln1-HAp or Flo8-HAp.

The regulation of translation initiation and the stability of mRNAs are intimately linked (41). We asked whether mutations in mRNA decapping or degradation enzymes affect the expression of *STE12*. Previously, our group reported that the deletion mutation of *KEM1*/*XRN1*, which encodes a major cytoplasmic 5′-3′ exoribonuclease, causes a defect in haploid invasive and diploid filamentous growth (18). *DHH1* encodes a DEAD box RNA helicase and has been reported to be an activator of decapping (8, 11). *DHH1* and *KEM1*/*XRN1* have been shown to be the components of the mRNA processing bodies (5, 25). Recent results suggest that Dhh1 also functions as a repressor of translation (7). The level of Ste12 protein was examined in the *dhh1*/*dhh1* and *kem1*/*kem1* mutant strains. As shown in Fig. 4A, the *kem1* mutation did not affect the level of Ste12 protein under filamentous-growth conditions. These results rule out the possibility that the *kem1* mutation affects the stability of *STE12* mRNAs and thus alters *STE12* expression. In the *dhh1*/*dhh1* mutant strains, the Ste12p level did not increase during filamentation. The level of Ste12p in *dhh1* mutant cells was 0.14 relative to that in the wild type (Fig. 4B). Northern blotting showed that the *caf20*, *dhh1*, and *tif1* mutations have no effect on *STE12-HA* transcripts (Fig. 4C). Our results suggest that *CAF20*, *DHH1*, and *TIF1* are required for *STE12* expression at the protein level during filamentous growth.

***caf20*/*caf20* and *dhh1*/*dhh1* mutants show defects in filamentous growth.** The transcription factor Ste12 is essential for activation of filamentation-specific genes. We investigated whether the low levels of Ste12 protein in *caf20*/*caf20*, *dhh1*/*dhh1*, and *tif1*/*tif1* mutant cells result in defects in filamentous growth. Pseudohyphal phenotypes of these mutant strains were tested. The colony morphologies on SLAD were examined before and after washing (Fig. 5A). The *caf20*/*caf20* mutants exhibited pseudohyphal colony morphology with an unusual colony edge. The differences from the wild type were more evident in the agar invasion phenotype. The *dhh1*/*dhh1* mutants were defective in the pseudohyphal colony morphologies and agar invasion phenotypes. The *tif1*/*tif1* mutants, however, did not show any defects in the pseudohyphal phenotypes.

We next examined the cellular morphologies on the SLAD plates by light microscopy (Fig. 5B). After 10 h, the colony-forming cells of the wild-type strain were elongated and formed pseudohyphae, whereas *caf20*/*caf20* and *dhh1*/*dhh1* cells were in the yeast form. These results indicate that *caf20*

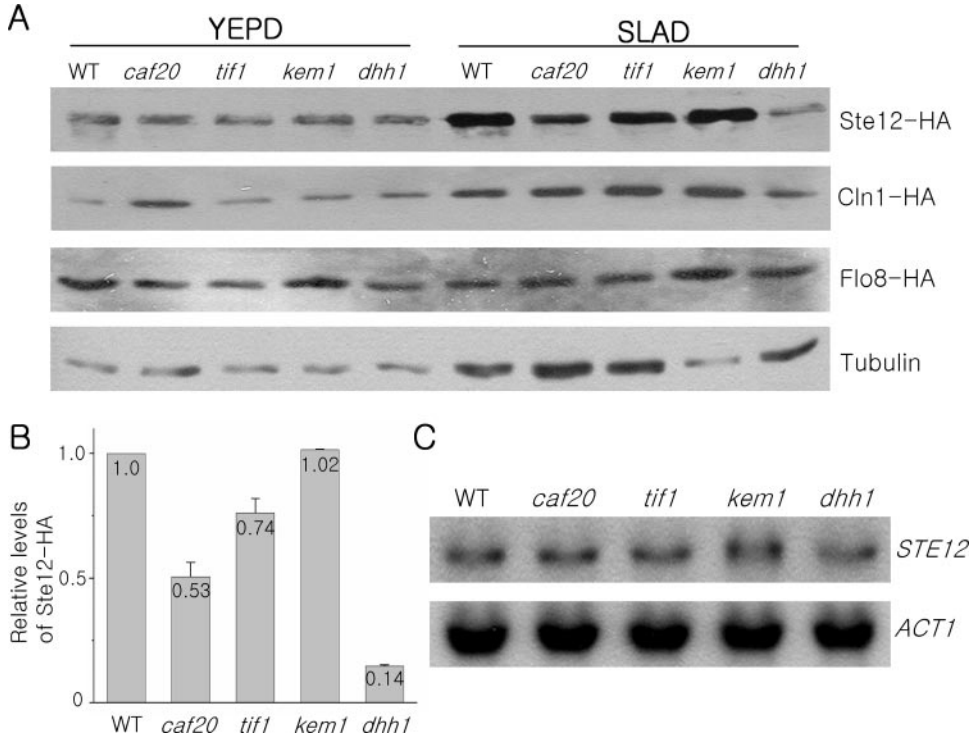

FIG. 4. Effects of *caf20*, *dhh1*, and *tif1* mutations on the induction of Ste12-HA protein during the pseudohyphal transition. (A) Western blots of Ste12-HA, Cln1-HA, and Flo8-HA. Plasmid pJI255 (STE12-HA), pJI256 (CLN1-HA), or pJI257 (FLO8-HA) was introduced into wild-type strain JK353 and mutant diploid strains JK383 (*caf20*/*caf20*), JK386 (*tif1*/*tif1*), JK354 (*kem1*/*kem1*), and JK389 (*dhh1*/*dhh1*). After growth for 8 h in YEPD medium or SLAD, total proteins were analyzed by Western blotting. (B) Relative levels of Ste12-HA protein in SLAD. The results are averages for three independent Western experiments. (C) Northern blots of *STE12-HA* in SLAD.

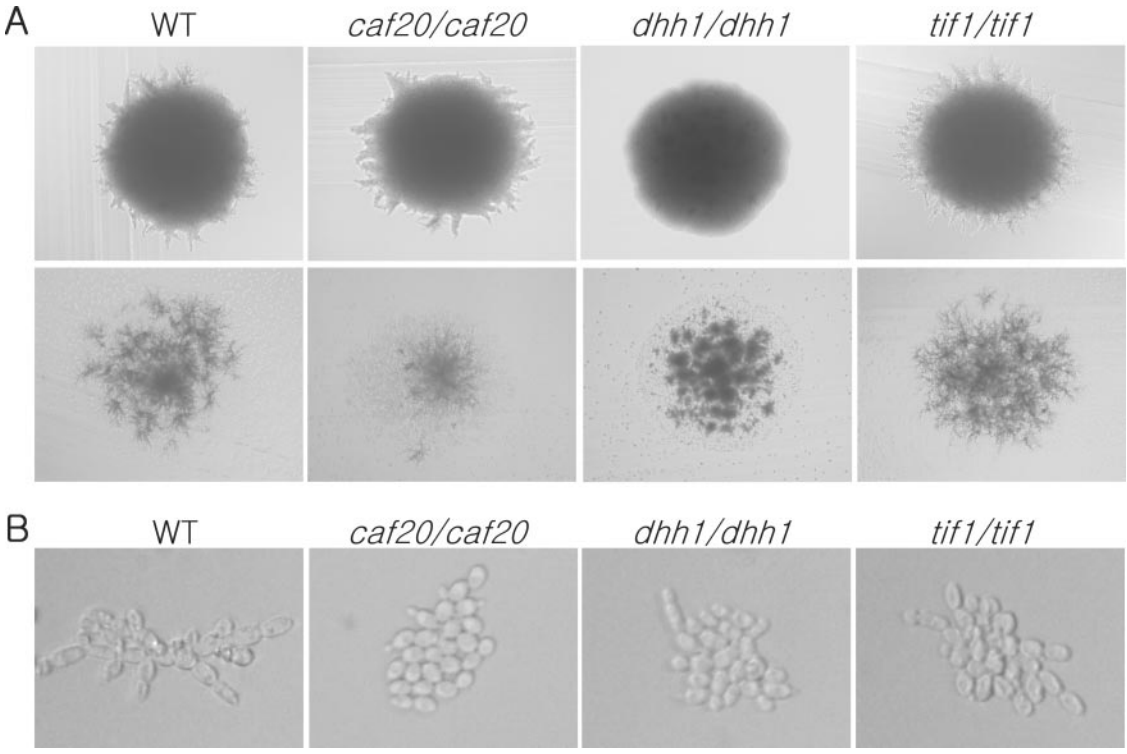

FIG. 5. Pseudohyphal defects of *caf20*/*caf20* and *dhh1*/*dhh1* mutant strains. (A) Colony morphologies. Wild-type strain JK353 and mutant strains JK383 (*caf20*/*caf20*), JK386 (*tif1*/*tif1*), and JK389 (*dhh1*/*dhh1*) were tested on SLAD plates. After 5 days of incubation, the colonies were photographed before (top) and after (bottom) cells were washed off the agar plate. (B) Enlarged view of the cells on the SLAD plate after 10 h of incubation.

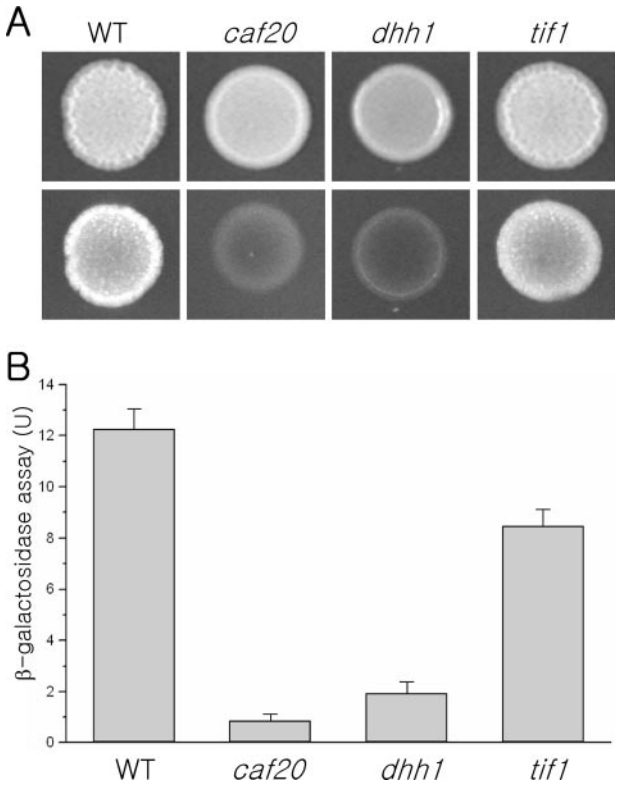

FIG. 6. Invasive-growth defect of *caf20* and *dhh1* mutants. (A) Wild-type strain 10560-2B and mutant strains JK381 (*caf20*), JK384 (*tif1*), and JK387 (*dhh1*) were tested on YEPD. Cell suspensions of each strain were applied to the plates and incubated for 3 days. The plates were photographed before and after cells were washed off the agar surface. (B) The β-galactosidase activities of plasmid *FLO11-lacZ* were measured in wild-type strain 10560-2B and mutant strains JK381 (*caf20*), JK384 (*tif1*), and JK387 (*dhh1*). β-Galactosidase assays were essentially the same as previously described (40).

and *dhh1* mutations show defects in pseudohyphal development.

Invasive growth of the haploid mutant strains was tested on YEPD medium (Fig. 6A). The *caf20* and *dhh1* mutants were markedly defective in invasive growth. The invasive growth of the *tif1* mutant, however, was similar to that of the wild type. The invasive-growth phenotypes of the mutant strains were in good correlation with *FLO11-lacZ* expression in the mutant cells (Fig. 6B). These results indicate that *CAF20* and *DHH1* play critical roles in both haploid invasive growth and diploid pseudohyphal development.

Filamentous growth defects caused by *caf20*/*caf20* and *dhh1*/*dhh1* mutations are suppressed by overexpression of *STE12*. To determine whether the overexpression of *STE12* suppresses the filamentation defects caused by *caf20* and *dhh1* mutations, we introduced a 2μ-based plasmid carrying *STE12* with its own promoter into diploid mutant strains. As shown in Fig. 7A, *STE12* overexpression restored both the filamentous colony morphology and the agar invasion phenotype to the *caf20*/*caf20* and *dhh1*/*dhh1* mutant strains. The level of Ste12p in each overexpressing strain, which was analyzed with the *STE12-HA* allele, was consistent with its suppression phenotype (Fig. 7B). *STE12* overexpression enhanced filamentation in the *caf20*/*caf20* strain to nearly the same extent as in the wild-type strain. *STE12* overexpression in the *dhh1*/*dhh1* strain, by contrast, only slightly enhanced filamentation and resulted in a reduced colony size. On the basis of these results, we propose that the filamentation phenotypes in the *caf20*/*caf20* and *dhh1*/*dhh1* mutant strains are closely related to their low levels of Ste12p.

DISCUSSION

The signaling pathways and the transcriptional regulations associated with filamentous growth of *S. cerevisiae* have been analyzed in considerable detail, but understanding of the regulation at the protein level is limited (14, 19, 21). Here, we identified three genes, *STE12*, *GPA2*, and *CLN1*, that are up-regulated at the protein level during the yeast-to-pseudohyphal-form transition. The increased levels of these proteins could be due to increased translation or greater protein stability. On the basis of our data, it is likely that these regulations are at the translational level. Polyribosomal mRNAs for *STE12*, *GPA2*, and *CLN1* were abundant under hyphal-culture conditions, indicating that they were actively translated. We also showed that Caf20, which is a cap-dependent translation inhibitor, is involved in the up-regulation of Ste12 protein during filamentous growth.

Our findings suggest for the first time that *CAF20* and *DHH1* participate in filamentous growth. The 4E-BPs, which were the first eIF4E-inhibitory proteins discovered, modulate eIF4E-eIF4G interaction by sequestering available eIF4E (35). In *S. cerevisiae*, Caf20 was found to be equivalent to 4E-BPs (2). Deletion of *CAF20* increases the growth rate in rich media and partially suppresses the effects of mutations in translation initiation factors (2, 9). In vitro translation assays show that p20 inhibits the translation of capped reporter mRNAs (2). There have been fewer studies on the significance of Caf20 as a cap-dependent translation repressor in *S. cerevisiae* than in cells of higher eukaryotes. Dhh1 was previously reported as a decapping activator but was recently shown also to function as a translational repressor (7, 8, 11). Our finding that the level of the Ste12 protein does not increase in the *caf20*/*caf20* or *dhh1*/*dhh1* mutant cells implies that Caf20 and Dhh1, previously known as general translational repressors, play positive roles in the up-regulation of Ste12 protein under filamentous-growth conditions.

The low level of Ste12p in *caf20*/*caf20* and *dhh1*/*dhh1* mutant cells appeared to be the main reason for the filamentation defects, because overexpression of *STE12* in *caf20*/*caf20* and *dhh1*/*dhh1* mutant cells restored the filamentation phenotypes. Each of these mutants, however, has a different phenotype. The *caf20*/*caf20* mutant strain showed a reduced invasiveness, whereas the *dhh1*/*dhh1* mutant strain had a more severe defect in filamentation. In addition, overexpression of *STE12* in the *dhh1*/*dhh1* mutant strain resulted in a synthetic phenotype (i.e., reduced colony size) (Fig. 7A). In the present study, we observed mainly a reduced level of Ste12p in the *caf20*/*caf20* or *dhh1*/*dhh1* mutant strains, but it remains possible that the *caf20* or *dhh1* mutation could affect expression of other filamentation-associated genes, such as *SFL1*, *TEC1*, etc. (29, 32). In addition, *DHH1* has been implicated in a number of cellular processes, including mRNA decapping, deadenylation, tran-

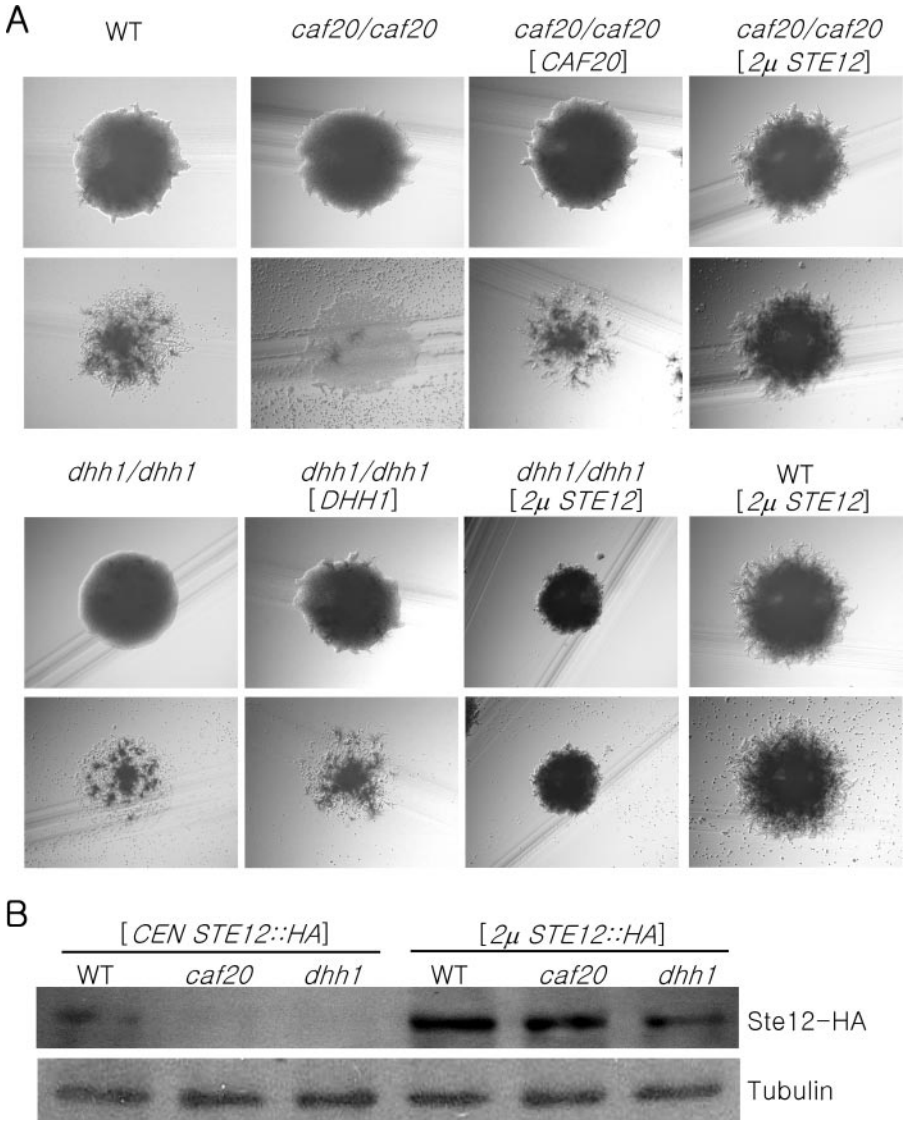

FIG. 7. Suppression of *caf20* and *dhh1* mutations by overexpression of *STE12*. (A) Pseudohyphal phenotypes of *caf20*/*caf20* and *dhh1*/*dhh1* mutant strains carrying the *STE12* overexpression plasmid. A wild-type strain (JK353) and mutant strains JK383 (*caf20*/*caf20*) and JK389 (*dhh1*/*dhh1*) were transformed with vector pRS426 or 2μ *STE12* (pJI274) and tested on SLAD plates. After 5 days of incubation, the colony morphology was photographed before (top) and after (bottom) cells were washed off the agar plate. The *caf20*/*caf20* strain with the *CAF20* plasmid (pJI276) and the *dhh1*/*dhh1* strain with the *DHH1* plasmid (pJI277) were also included. (B) Ste12p levels in *caf20*/*caf20* and *dhh1*/*dhh1* mutant strains carrying the *STE12* overexpression plasmid. Wild-type strain JK353 and mutant strains JK383 (*caf20*/*caf20*) and JK389 (*dhh1*/*dhh1*) carrying either pJI255 (*CEN STE12*::*HA*) or pJI274 (2μ *STE12*::*HA*) were grown for 8 h in SLAD. Total proteins were analyzed by Western blotting.

scription, and G_1/S cell cycle arrest (4, 8). Further analysis of the role of *CAF20* and *DHH1* in filamentous growth and *STE12* expression, therefore, should help clarifying their roles in yeast cells.

Three genes, *STE12*, *GPA2*, and *CLN1*, were identified in our screening as genes that are up-regulated at the protein level during filamentous growth. We observed that the *caf20* and *dhh1* mutations did not affect the level of Cln1p. These results imply that the up-regulation of *CLN1* mRNA translation is independent of *CAF20* and *DHH1*. The Cln1p level appeared to be further increased by the *STE11-4* hyperactive allele under the filamentous-growth conditions, whereas the Ste12p level was not affected by this allele (data not shown). These results suggest that different mechanisms regulate *CLN1* and *STE12* expression. We are currently investigating other components of the translation initiation and mRNA decay pathways that appear to participate in translational regulation during filamentation.

ACKNOWLEDGMENTS

We thank Gerald. R. Fink and Haoping Liu for strains and plasmids and Alan G. Hinnebusch for helpful advice on polyribosome fractionation.

This work was supported by a grant from the Korean Science and Engineering Foundation (R04-2000-000-00040-0) and the Korea Research Foundation Grant, funded by the Korean Government (MOEHRD) (KRF-2004-041-C00350), to J. Kim.

REFERENCES

1. **Adams, A., D. E. Gottschling, C. A. Kaiser, and T. Stearn.** 1997. Methods in yeast genetics. Cold Spring Harbor Press, Cold Spring Harbor, N.Y.
2. **Altmann, M., N. Schmitz, C. Berset, and H. Trachsel.** 1997. A novel inhibitor of cap-dependent translation initiation in yeast: p20 competes with eIF4G for binding to eIF4E. EMBO J. **16:**1114–1121.
3. **Arava, Y., Y. Wang, J. D. Storey, C. L. Liu, P. O. Brown, and D. Herschlag.** 2003. Genome-wide analysis of mRNA translation profiles in *Saccharomyces cerevisiae*. Proc. Natl. Acad. Sci. USA **100:**3889–3894.
4. **Bergkessel, M., and J. C. Reese.** 2004. An essential role for the *Saccharomyces cerevisiae* DEAD-box helicase *DHH1* in G1/S DNA-damage checkpoint recovery. Genetics **167:**21–33.
5. **Brengues, M., D. Teixeira, and R. Parker.** 2005. Movement of eukaryotic mRNAs between polysomes and cytoplasmic processing bodies. Science **310:** 486–489.
6. **Christianson, T. W., R. S. Sikorski, M. Dante, J. H. Shero, and P. Hieter.** 1992. Multifunctional yeast high-copy-number shuttle vectors. Gene **110:** 119–122.
7. **Coller, J., and R. Parker.** 2005. General translational repression by activators of mRNA decapping. Cell **122:**875–886.
8. **Coller, J. M., M. Tucker, U. Sheth, M. A. Valencia-Sanchez, and R. Parker.** 2001. The DEAD box helicase, Dhh1p, functions in mRNA decapping and interacts with both the decapping and deadenylase complexes. RNA **7:**1717–1727.
9. **de la Cruz, J., I. Iost, D. Kressler, and P. Linder.** 1997. The p20 and Ded1 proteins have antagonistic roles in eIF4E-dependent translation in *Saccharomyces cerevisiae*. Proc. Natl. Acad. Sci. USA **94:**5201–5206.
10. **Elder, R. T., E. Y. Loh, and R. W. Davis.** 1983. RNA from the yeast transposable element Ty1 has both ends in the direct repeats, a structure similar to retrovirus RNA. Proc. Natl. Acad. Sci. USA **80:**2432–2436.
11. **Fischer, N., and K. Weis.** 2002. The DEAD box protein Dhh1 stimulates the decapping enzyme Dcp1. EMBO J. **21:**2788–2797.
12. **Foiani, M., A. M. Cigan, C. J. Paddon, S. Harashima, and A. G. Hinnebusch.** 1991. *GCD2*, a translational repressor of the *GCN4* gene, has a general function in the initiation of protein synthesis in *Saccharomyces cerevisiae*. Mol. Cell. Biol. **11:**3203–3216.
13. **Gagiano, M., D. van Dyk, F. F. Bauer, M. G. Lambrechts, and I. S. Pretorius.** 1999. Msn1p/Mss10p, Mss11p and Muc1p/Flo11p are part of a signal transduction pathway downstream of Mep2p regulating invasive growth and pseudohyphal differentiation in *Saccharomyces cerevisiae*. Mol. Microbiol. **31:**103–116.
14. **Gancedo, J. M.** 2001. Control of pseudohyphae formation in *Saccharomyces cerevisiae*. FEMS Microbiol. Rev. **25:**107–123.
15. **Gavrias, V., A. Andrianopoulos, C. J. Gimeno, and W. E. Timberlake.** 1996. *Saccharomyces cerevisiae TEC1* is required for pseudohyphal growth. Mol. Microbiol. **19:**1255–1263.
16. **Gimeno, C. J., P. O. Ljungdahl, C. A. Styles, and G. R. Fink.** 1992. Unipolar cell divisions in the yeast *S. cerevisiae* lead to filamentous growth: regulation by starvation and RAS. Cell **68:**1077–1090.
17. **Guo, B., C. A. Styles, Q. Feng, and G. R. Fink.** 2000. A *Saccharomyces* gene family involved in invasive growth, cell-cell adhesion, and mating. Proc. Natl. Acad. Sci. USA **97:**12158–12163.
18. **Kim, J.** 2002. *KEM1* is involved in filamentous growth of *Saccharomyces cerevisiae*. FEMS Microbiol. Lett. **216:**33–38.
19. **Köhler, T., S. Wesche, N. Taheri, G. H. Braus, and H. U. Mosch.** 2002. Dual role of the *Saccharomyces cerevisiae* TEA/ATTS family transcription factor Tec1p in regulation of gene expression and cellular development. Eukaryot. Cell **1:**673–686.
20. **Law, G. L., K. S. Bickel, V. L. MacKay, and D. R. Morris.** 2005. The undertranslated transcriptome reveals widespread translational silencing by alternative 5′ transcript leaders. Genome Biol. **6:**R111.
21. **Liu, H., C. A. Styles, and G. R. Fink.** 1993. Elements of the yeast pheromone response pathway required for filamentous growth of diploids. Science **262:** 1741–1744.
22. **Liu, H., C. A. Styles, and G. R. Fink.** 1996. *Saccharomyces cerevisiae* S288C has a mutation in *FLO8*, a gene required for filamentous growth. Genetics **144:**967–978.
23. **Lo, W. S., and A. M. Dranginis.** 1998. The cell surface flocculin Flo11 is required for pseudohyphae formation and invasion by *Saccharomyces cerevisiae*. Mol. Biol. Cell **9:**161–171.
24. **Loeb, J. D., T. A. Kerentseva, T. Pan, M. Sepulveda-Becerra, and H. Liu.** 1999. *Saccharomyces cerevisiae* G1 cyclins are differentially involved in invasive and pseudohyphal growth independent of the filamentation mitogen-activated protein kinase pathway. Genetics **153:**1535–1546.
25. **Long, R. M., and M. T. McNally.** 2003. mRNA decay: x (*XRN1*) marks the spot. Mol. Cell **11:**1126–1128.
26. **Lorenz, M. C., and J. Heitman.** 1997. Yeast pseudohyphal growth is regulated by *GPA2*, a G protein alpha homolog. EMBO J. **16:**7008–7018.
27. **Lorenz, M. C., R. S. Muir, E. Lim, J. McElver, S. C. Weber, and J. Heitman.** 1995. Gene disruption with PCR products in *Saccharomyces cerevisiae*. Gene **158:**113–117.
28. **MacKay, V. L., X. Li, M. R. Flory, E. Turcott, G. L. Law, K. A. Serikawa, X. L. Xu, H. Lee, D. R. Goodlett, R. Aebersold, L. P. Zhao, and D. R. Morris.** 2004. Gene expression analyzed by high-resolution state array analysis and quantitative proteomics: response of yeast to mating pheromone. Mol. Cell. Proteomics **3:**478–489.
29. **Madhani, H. D., T. Galitski, E. S. Lander, and G. R. Fink.** 1999. Effectors of a developmental mitogen-activated protein kinase cascade revealed by expression signatures of signaling mutants. Proc. Natl. Acad. Sci. USA **96:** 12530–12535.
30. **Madhani, H. D., C. A. Styles, and G. R. Fink.** 1997. MAP kinases with distinct inhibitory functions impart signaling specificity during yeast differentiation. Cell **91:**673–684.
31. **Pan, X., and J. Heitman.** 1999. Cyclic AMP-dependent protein kinase regulates pseudohyphal differentiation in *Saccharomyces cerevisiae*. Mol. Cell. Biol. **19:**4874–4887.
32. **Pan, X., and J. Heitman.** 2002. Protein kinase A operates a molecular switch that governs yeast pseudohyphal differentiation. Mol. Cell. Biol. **22:**3981–3993.
33. **Pestova, T. V., and C. U. Hellen.** 2001. Functions of eukaryotic factors in initiation of translation. Cold Spring Harbor Symp. Quant. Biol. **66:**389–396.
34. **Ramirez, M., R. C. Wek, and A. G. Hinnebusch.** 1991. Ribosome association of GCN2 protein kinase, a translational activator of the *GCN4* gene of *Saccharomyces cerevisiae*. Mol. Cell. Biol. **11:**3027–3036.
35. **Richter, J. D., and N. Sonenberg.** 2005. Regulation of cap-dependent translation by eIF4E inhibitory proteins. Nature **433:**477–480.
36. **Roberts, R. L., and G. R. Fink.** 1994. Elements of a single MAP kinase cascade in *Saccharomyces cerevisiae* mediate two developmental programs in the same cell type: mating and invasive growth. Genes Dev. **8:**2974–2985.
37. **Rupp, S., E. Summers, H. J. Lo, H. Madhani, and G. R. Fink.** 1999. MAP kinase and cAMP filamentation signaling pathways converge on the unusually large promoter of the yeast *FLO11* gene. EMBO J. **18:**1257–1269.
38. **Sambrook, J., E. F. Fritsch, and T. Maniatis.** 1989. Molecular cloning: a laboratory manual, 2nd ed. Cold Spring Harbor Laboratory Press, Cold Spring Harbor, N.Y.
39. **Schmid, S. R., and P. Linder.** 1991. Translation initiation factor 4A from *Saccharomyces cerevisiae*: analysis of residues conserved in the D-E-A-D family of RNA helicases. Mol. Cell. Biol. **11:**3463–3471.
40. **Schneider, S., M. Buchert, and C. M. Hovens.** 1996. An in vitro assay of beta-galactosidase from yeast. BioTechniques **20:**960–962.
41. **Sheth, U., and R. Parker.** 2003. Decapping and decay of messenger RNA occur in cytoplasmic processing bodies. Science **300:**805–808.
42. **Sikorski, R. S., and P. Hieter.** 1989. A system of shuttle vectors and yeast host strains designed for efficient manipulation of DNA in *Saccharomyces cerevisiae*. Genetics **122:**19–27.
43. **von der Haar, T., and J. E. McCarthy.** 2002. Intracellular translation initiation factor levels in *Saccharomyces cerevisiae* and their role in cap-complex function. Mol. Microbiol. **46:**531–544.
44. **Wach, A., A. Brachat, R. Pohlmann, and P. Philippsen.** 1994. New heterologous modules for classical or PCR-based gene disruptions in *Saccharomyces cerevisiae*. Yeast **10:**1793–1808.
45. **Zong, Q., M. Schummer, L. Hood, and D. R. Morris.** 1999. Messenger RNA translation state: the second dimension of high-throughput expression screening. Proc. Natl. Acad. Sci. USA **96:**10632–10636.